V

VERTICAL SEISMIC PROFILING

James W. Rector, III[1], Maria-Daphne Mangriotis[2]
[1]Department of Civil and Environmental Engineering, University of California at Berkeley, Berkeley, CA, USA
[2]Applied Geophysics, Institute of Engineering Seismology and Earthquake Engineering (ITSAK), Thessaloniki, Greece

Synonyms

VSP

Definition

Vertical Seismic Profiling A geophysical technology for measuring the *seismic* properties in a *profile* of the earth using a set of sources and receivers, either of which are placed along the depth (*vertical*) axis.

Introduction

Vertical seismic profiling (commonly abbreviated to the name VSP) is a major technique in geophysical exploration, which involves measuring downgoing and upgoing seismic wavefields through a stratigraphic sequence. Shortly after the first attempts of developing surface reflection seismology, where both sources and receivers were at the surface, the line of research set out with the idea of burying either sources or receivers in boreholes. McCollum and LaRue (1931) proposed that local geologic structure could be determined from measuring the arrival of seismic energy from surface sources with buried receivers. This geometry forms the basic principle of determining seismic wave propagation velocities from VSP measurements even today. The technology of VSP acquisition and processing was initially developed by researchers in the former Soviet Union in the 1950s through the 1970s. It was only later, in the mid 1970s, that non-Soviet geophysicists became systematically engaged in the advance of VSP technology for exploration applications. Today, the fruits of these efforts have served not only in the improvement of velocity analysis, but have materialized numerous other applications ranging from structural imaging of complex 3D structures such as faults and salt domes in exploration studies, to directing drill operations, monitoring secondary recovery processes, and hydraulic fracturing.

Acquisition techniques

A variety of data acquisition techniques are currently employed, depending on the survey's application and financial budget. Figure 1 shows the main geometric configurations, which include (1) zero-offset VSP (ZVSP), where the source is near the well-head above the vertical receiver array, (2) offset VSP, where the source is located a distance away from the vertical borehole, (3) multi-offset VSP, for multiple distances of the source to the borehole, (4) walk-away VSP, where multiple sources are located on a line at the surface and the receivers in a vertical array, (5) walk-above VSP, where the sources are located over receivers buried in a deviated or horizontal well, and (6) drill-bit SWD (seismic while drilling) VSP, where the drill-bit acts as the seismic source and the receivers are on the surface. 3D VSP uses borehole receivers, and a 2D surface source geometry (i.e., multi-azimuth multi-offset, or walk-away VSP).

The common active seismic sources used in VSP include those used in land and marine surface studies (see *Seismic Data Acquisition and Processing*) as well as the noise of the drill-bit in the case of SWD-VSP. There is a variety of geophone tools available for use in cased or uncased boreholes, which combine three orthogonal geophones, a hydrophone and other borehole seismic tools at each recording level. The receiver spacing is set by the depth-sampling interval to avoid spatial aliasing.

Harsh K. Gupta (ed.), *Encyclopedia of Solid Earth Geophysics*, DOI 10.1007/978-90-481-8702-7,

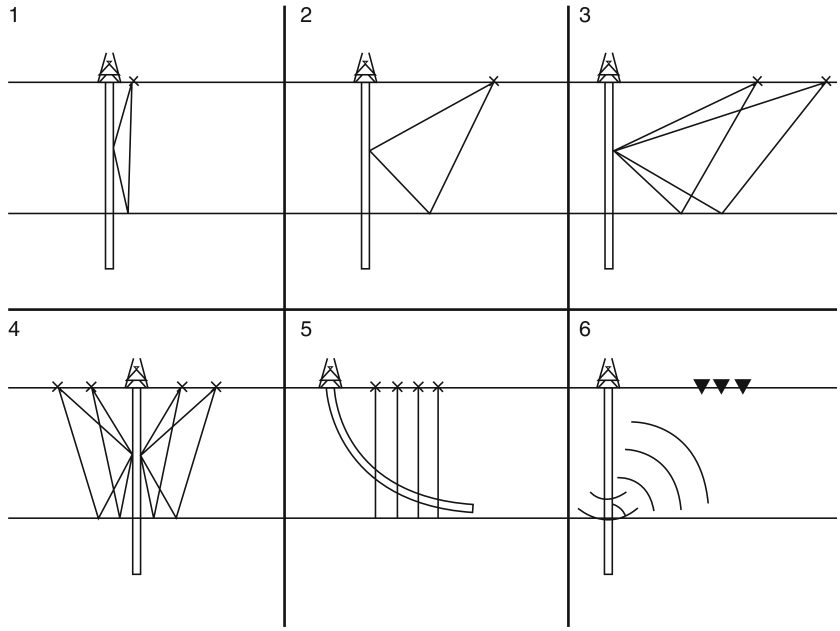

Vertical Seismic Profiling, Figure 1 Common acquisition geometries for vertical seismic profiling (VSP): (1) zero-offset VSP (ZVSP), (2) offset VSP, (3) multi-offset VSP, (4) walk-away VSP, (5) walk-above VSP, and (6) drill-bit SWD (seismic while drilling) VSP.

To limit field acquisition time, most commonly multilevel receiver arrays are employed. The main source of noise in VSP studies are tube waves, which are generated when the fluid in the well is displaced by a seismic source, such as ground roll. Tube waves propagate up and down a well and create secondary tube waves in borehole anomalies, which may interfere with primary reflections. As a coherent noise mode, tube waves cannot be attenuated by stacking, therefore, both field procedures, such as use of attenuating heavy mud and construction of ditches to attenuate the ground roll, as well as processing techniques, such as filtering and tube wave modeling, are commonly used to minimize their effect.

VSP applications

The primary use of VSP is the integration of VSP and downhole logging to surface reflection surveys (Hardage, 1985). Contrary to surface studies, which infer subsurface conditions from measurement of the reflected wavefields with the source and receiver at the surface, a VSP configuration involves closely spaced direct physical measurements of the wavefield between the source position and the reflector.

Zero-offset VSP measurements can be correlated with sonic logs and check-shot surveys in the borehole and improve the depth positioning of reflections recorded in surface data. From a velocity perspective, zero-offset VSP measurements are denser than check-shot surveys; hence, they provide a finer interval velocity profile. On the other hand, VSP samples a larger velocity body around the well than the high frequency sonic log, which may be subject to cycle skipping and the effects of the washed-out zones. VSP also contains the signature of the near-surface, which is often absent in logging. Hence, synthetic seismograms computed from sonic logs may not accurately represent reflections recorded from surface measurements. Reflections from zero-offset VSP, however, can be matched to those from surface measurements via an appropriate static time-shift to account for the differential travel times of the two recording geometries.

Concerning seismic imaging, the recorded wavefield in a buried VSP array has higher signal to noise ratio across a larger seismic bandwidth than surface measurements for two reasons. First, surface cultural noise is suppressed in the borehole, and second, upgoing reflections do not propagate through the near-surface material, which is highly *attenuating* (see *Seismic, Viscoelastic Attenuation*). In addition, the reflections recorded in a VSP suffer less attenuation as the distance to the target is shorter. This shorter distance also implies that the *Fresnel zone* (see *Seismic, Waveform Modeling and Tomography*) is smaller in the case of a VSP, leading to higher resolution compared to surface seismic studies. Given that downgoing and upgoing wave modes are separated in the f-k space, either an f-k filter, or a trace by trace arithmetic subtraction of the estimated wave mode can isolate downgoing from upgoing waves. Estimation of the downgoing wavefield from VSP data is used in the design of deconvolution operators, which can be thereafter applied to surface data to improve the vertical resolution. On the other hand, upgoing reflections can be mapped to their origin position via either a CDP-VSP mapping, or *Seismic, Migration* algorithm, or a combination of the two. A migration step is strongly advisable in the case of complex geologies. In recent years, VSP seismic imaging has transformed from an analysis of acoustic reflections to migrating converted-wave reflections (Grech et al., 2001), which may be more sensitive to imaging tight-sand reservoirs compared to P-P reflections (O'Brien and Harris, 2006), as well as to applications of free-surface multiples, which can increase the narrow cone of coverage of a VSP to that of a 3D CDP survey (Jiang et al., 2005). Another promising technique for seismic imaging applications is interferometric imaging, which through the creation of virtual sources (VS) in the location of the receivers eliminates the need for any knowledge of the complex overburden (Bakulin and Calvert, 2004). In addition, unlike traditional migration schemes, interferometric imaging circumvents a priori knowledge of the velocity structure in the vicinity of targets, such as salt flanks, and can be applied to imaging complex structures above or below a receiver array (Xiao et al., 2006; Vasconcelos et al., 2008).

Through the separation of downgoing and upgoing wavefields and their relative amplitudes, it is possible to extract the true *reflection coefficients* (see *Energy Partitioning of Seismic Waves*) used for lithological interpretation. Moreover, from multi-offset 3-component VSP data it is possible to determine the *AVO response* (see *Energy Partitioning of Seismic Waves*) with no assumptions to the path of the propagating wavefield, which is required in surface seismic AVO analysis.

Another benefit of using VSP measurements is their robustness in estimating *Seismic Anisotropy*, which improves lithologic interpretations as well as increases the quality of seismic imaging. Given the seismic velocity response to changes in reservoir porosity and fluid content, velocity *Seismic Anisotropy* can also be applied in monitoring of fluid-drainage patterns during production. Fracturing will also affect seismic velocity; hence, VSP velocity measurements can also be used in monitoring hydraulic fracturing.

With *attenuation* (see *Seismic, Viscoelastic Attenuation*) gaining increasing importance as a seismic parameter linked to lithological properties, VSP has proven to be a powerful tool for *Q* (see *Seismic, Viscoelastic Attenuation*) estimation. Aside from true amplitude processing required in stratigraphic interpretation, VSP-derived Q profiles are also used in the design of inverse Q-filters to enhance seismic resolution. Recent studies also suggest a link between anisotropic attenuation and fracturing (Maultzsch et al., 2007); hence, VSP azimuthal measurements of attenuation may potentially be applied in monitoring hydraulic fracturing in hydrocarbon and geothermal applications.

Summary

In recent years, VSP surveys are becoming increasingly popular for reducing risk in well placement and improving reservoir monitoring. Intrinsic to the complex geometry of the VSP, which poses several data acquisition and processing challenges, is the ability of the VSP to expand the spatial and time-lapse subsurface characterization potential of conventional downhole logging and surface reflection studies. Henceforth, following the success of VSP surveys and their increased benefits over their financial cost, the VSP technique is a rapidly developing area of geophysical research and may soon become a standard logging service.

Bibliography

Kirtland Grech, M. G., Lawton, D. C., and Cheadle, S., 2001. Integrated Pre-stack Depth Migration of VSP and Surface Seismic Data. CSEG, Calgary, Alberta, Canada, November Issue: 50–56.

Bakulin, A., and Calvert, R., 2004. Virtual Source: New Method for Imaging and 4D Below Complex Overburden. *Society of Exploration Geophysicists Expanded Abstracts*, **23**, 2477–2481.

Hardage, B. A., Helbig, K., and Treitel, S., 1985. Vertical Seismic Profiling, *Handbook of Geophysical Exploration, Seismic Exploration*: Geophysical Press. Elsevier Science Ltd, The Boulevard, Langford Lane, Kidlington, Oxford, OX5, GB, UK.

Jiang, Z., Yu, J., and Schuster, G. T., 2005. Migration of multiples. *The Leading Edge*, **24**, 315–318.

Maultzsch, S., Chapman, M., Liu, E., and Li, X.-Y., 2007. Modeling and analysis of attenuation anisotropy in multi-azimuth VSP data from the clair field. *Geophysical Prospecting*, **55**, 627–642.

McCollum, B., and LaRue, W. W., 1931. Utilization of existing wells in seismograph work. *Early Geophysical Papers*, **1**, 119–127.

O'Brien, J., and Harris, R., 2006. Multicomponent VSP imaging of tight-gas sands. *Geophysics*, **71**, 83–90.

Vasconcelos, I., Snieder, R., and Hornby, B., 2008. Imaging of internal muliples from subsalt VSP data – Examples of target-oriented interferometry. *Geophysics*, **73**, 157–168.

Xiao, X., Zhou, M., and Schuster, G. T., 2006. Salt-flank delineation by interferometric imaging of transmitted P- to S-waves. *Geophysics*, **71**, 197–207.

Cross-references

Energy Partitioning of Seismic Waves
Seismic Anisotropy
Seismic Data Acquisition and Processing
Seismic, Migration
Seismic, Viscoelastic Attenuation
Seismic, Waveform Modeling and Tomography

VERY LONG BASELINE INTERFEROMETRY

Helmut Wiesemeyer[1], Axel Nothnagel[2]
[1]Millimeter and Submillimeter Astronomy, Max-Planck-Institute for Radio Astronomy, Bonn, Germany
[2]VLBI Research Group, Institute of Geodesy and Geoinformation, University of Bonn, Bonn, Germany

Synonyms

VLBI

Definition

Very Long Baseline Interferometry (VLBI). correlation interferometry of celestial objects with separately

operating radio antennas equipped with frequency standards, off-line data reduction remotely by a digital correlator.
e-VLBI. VLBI with transmission of data by a high-speed network instead of storage media.

Introduction

Very long baseline interferometry (VLBI) is a radio-astronomical technique to achieve high spatial resolution in astronomical imaging (of the order of milliarcseconds), involving antennas separated by thousands of kilometers (a "VLBI network"). Because the reconstruction of the image depends on the precise knowledge of the vector (hereafter: baseline) connecting the two antennas of a station pair, the a priori knowledge of the image can be used to determine the baseline vector by inverting the measurement equation, with a precision corresponding to a fraction of the wavelength. Such an a priori knowledge is naturally given if the astronomical source on the sky is spatially unresolved and therefore a "point source." Such sources – usually quasars, that is, the nuclei of bright radio galaxies – are spread over the entire sky and regularly observed in radio astronomy. Whereas VLBI in radio astronomy aims at resolving these active galactic nuclei, improper assumptions about source structure limit the accuracy of the determinations of antenna stations. This can be avoided by using appropriate source structure models (Tornatore and Charlot, 2007). The importance of VLBI techniques in Geophysics is evident if the two antennas of a baseline are located on different tectonic plates, whose relative motion and deformation can therefore be determined with high accuracy (qv *Geoid*).

A VLBI array can be thought as a fictive giant single-dish telescope whose aperture is synthesized while the baseline vector sweeps the sky thanks to the rotation of the Earth. The resulting image therefore depends on the angular momentum vector of the Earth. This dependency implies applications of VLBI in the measurements of the Earth's spin axis in space and with respect to the solid crust as well as irregularities of the *Earth Rotation*. Other, less precise methods are position determinations with the Global Positioning System (qv *GPS, Tectonic Geodesy*) and synthetic aperture radar measurements (qv *SAR Interferometry*), the latter being an interferometric method, like VLBI.

Methods and techniques in very long baseline interferometry

The idea of connecting several telescopes to an array in order to synthesize part of the surface of a single, large telescope dates back to 1946, when Ryle and Vonberg (1946) used for the first time a multi-element radio telescope for solar observations. In both optical and radio astronomy, the idea turned out to be extremely fruitful for achieving the highest spatial resolutions. For a single telescope, the resolution (in radians) is given by the ratio of wavelength to aperture diameter (up to a factor of order unity). By consequence, a radio telescope working at a wavelength of 21 cm needs an aperture of about 50 km in order to achieve the same angular resolution as, for example, an optical telescope limited by atmospheric seeing. The largest, fully steerable radio telescopes have apertures of the order of 100 m and reach, at that wavelength, an angular resolution of 9 arc minutes. As an alternative to even larger single-dish radio telescopes, several telescopes can be connected by microwave or fiber optics cables in order to form a connected-element interferometer. If the telescopes of such an interferometer are suitably distributed, a sufficiently long observation of a celestial source can be reconstructed to form an image whose angular resolution is of the order of the ratio of the wavelength to the longest among the distance vectors ("baseline," see Figure 1) between telescope pairs. The advantage of connected-element interferometers is that the signals can be correlated in real time, such that the phase of the electromagnetic wave when it arrives at the different telescopes is preserved. This is achieved by mixing the incoming signal with that from a local oscillator. In a connected-element interferometer, the local oscillators in all antennas are driven with a common phase reference. The Very Large Array (VLA, New Mexico) and the British e-Merlin array have elements connected by optical fiber cables, with baselines of up to 50 km (VLA) and 200 km (e-Merlin). Despite modern communication technology sometimes used (e.g., satellite links), the physical connection of array elements becomes impractical beyond a certain limit.

The step from a connected-element interferometer to a VLBI experiment consists of abandoning (for practical and economical reasons) the microwave or optical fiber links, registering the data, together with time marks, on a suitable storage medium, and analyzing the data later with a digital correlator. While local oscillators are necessary to convert the observed frequency band pass to one at a lower frequency (for recording the data), they cannot be locked to a common phase reference because of the large separation between the antennas. Time marks are therefore necessary. This technique became feasible with the availability of reliable frequency standards for the time marks, and magnetic tapes of sufficient storage capacity. The first VLBI observation correlated the data of a single baseline between the Hat Creek (California) and Green Bank (West Virginia) observatories (Bare et al., 1967). Since then, the major improvements in VLBI were mainly due to the increase of baseline length (i.e., spatial resolution) and collecting area (i.e., sensitivity), and due to the availability of more reliable clocks and faster digital samplers, leading to larger spectral bandwidth and thus sensitivity. Nowadays, hydrogen masers are used as frequency standards, while arrays of hard disks replace the tapes. The distinction between a connected-element interferometer and a VLBI network is somewhat imprecise. Using network connections of large bandwidth, VLBI data can now be transmitted in real time to the central correlator, while the local oscillators of the antennas participating in the

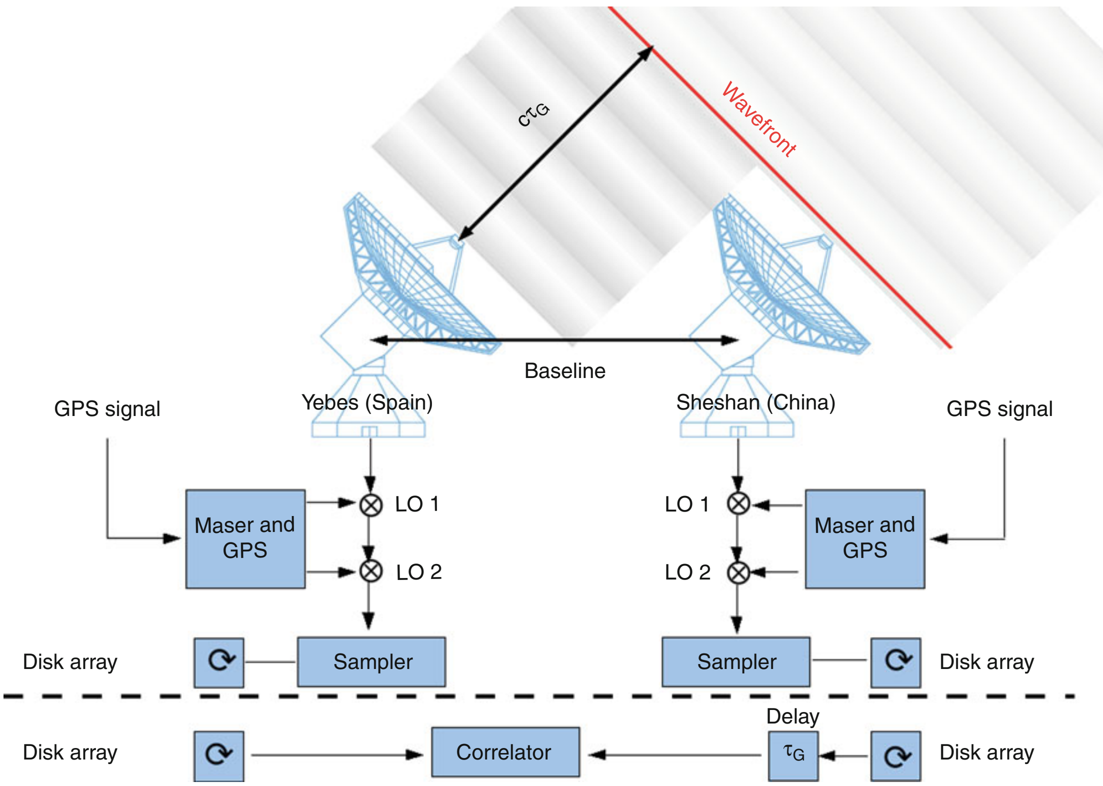

Very Long Baseline Interferometry, Figure 1 Schematic representation of an antenna pair on a baseline between Spain and China (distances not to scale). The electromagnetic wave from a distant point source (a quasar) is shown together with the position of the wave front when arriving in China (red line). The signal path corresponding to the time delay τ_G is shown, as well as the correction for the latter in the data reduction. There is no physical connection between both antennas, each operating with an independent local oscillator (labeled LO). The dashed line separates the measurement from the off-line data processing. Credits: Greve/IRAM/Rebus.

network are not synchronized. This technique has been demonstrated in 2005 with the European VLBI Network (EVN), involving a transatlantic baseline.

Physical principles

Interferometric experiments detect both amplitude and phase of electromagnetic waves (conveniently described by complex functions) and combine them in a suitable way to provide images, spectra, and polarization information. Phase-sensitive detection is possible by measuring correlations (or coherence functions) in the incoming electromagnetic field. It has been shown (Sudarshan, 1963) that for the case of two-point correlation functions, classical and quantum electrodynamics lead to equivalent results if nonlinear effects are ignored. We therefore limit our discussion to the case of ensembles of incoherent packets of quasi-monochromatic electromagnetic waves from different directions but confined to a small field of view.

The starting point of any interferometric imaging experiment is the van Cittert-Zernicke theorem (van Cittert, 1934; Zernike, 1938), stating that the correlation of the electromagnetic field at two points (two-point or mutual coherence function) is, up to a complex scaling factor, given by the Fourier transform (also called "visibility function") of the spatial intensity distribution (example: the interference pattern observed on a screen behind an illuminated slit or a grid). The complex scaling factor involves a correction due to the fact that the antenna baselines are not parallel to the plane of the sky (and, for the case of VLBI, not coplanar among them). This so-called delay correction τ_G needs to be applied because of the lag between the arrival times of the front of the electromagnetic wave at the antennas of a given baseline (Figure 1), and is equivalent to steering the fictive large single-dish telescope mentioned above to the source. The applied delay correction will differ from the theoretical one, owing to the clock error and to the inaccuracy of the assumed baseline length. In the absence of an error-free, absolute time scale, the data streams from an antenna pair rather have to be synchronized by maximizing the correlated signal, applying reasonably guessed delay corrections. A first synchronization is done by using the GPS time signal (qv *GPS, Data Acquisition and Analysis*) to which the local oscillators in the antennas are locked. A refinement needs to be applied later when the data are cross-correlated. There are actually two free parameters per baseline pair, not only the delay correction, but also the frequency of the oscillations, due to the Earth's rotation, in the interference pattern ("fringes"). This frequency has to be fitted, too, because it depends on the clock rate. For hydrogen masers, whose radio signal at a frequency of 1.4 MHz is now commonly used as a frequency standard for VLBI experiments, the fractional frequency drift (e.g., due to temperature drifts) after 100 s is of the order of 10^{-14}. Such a high precision is required if phase information is to be extracted once the signals are correlated. There is yet another difference between a connected-element interferometer with baselines of up to 10^6 wavelengths, and a VLBI experiment: in the former case, the field of view of the interferometer is limited by the central lobe of the antenna reception pattern ("main beam"), whereas in VLBI the field of view is limited by the largest delay τ_G within which the signal from a given direction is coherent. This delay depends on the baseline length with respect to the wavelength, on the spectral bandwidth across which these signals are averaged, and on the accuracy required (e.g., astrometry or precise baseline determinations need a higher degree of coherence). Therefore, the field of view of VLBI observations is much smaller than that of observations with connected-element interferometers. However, nowadays more evolved data analysis techniques exist that permit to overcome this limitation (Garrett et al., 1999).

For each telescope of the VLBI network, the data from the receiving system are recorded on an array of hard disks, together with the time marks from the clock. Later these data are correlated with a digital correlator. Modern correlators currently used are the Mark IV and Mark V or K4 and K5 systems. They allow us to analyze VLBI data for large frequency bands (for high sensitivity to continuum signals) or high-frequency resolution (for observing spectral lines).

Data calibration and imaging

After applying the aforementioned delay and fringe rate corrections, the phases of the complex data need to be recovered. The visibility functions are first smoothed to an integration time interval, which depends on the tolerated "visibility smearing": owing to the rotation of the Earth during this time span, different spatial frequencies are measured at different times, even for a single baseline. Furthermore, at the highest frequencies, where atmospheric fluctuations become important (mm VLBI), the elementary integration times are kept below 20 s, which allows one to apply atmospheric phase corrections. Another upper limit to the integration time interval is given by the stability of the clock. However, the time constant of a hydrogen maser is longer than the two previous limitations.

Unlike connected-element interferometers, where the phase of the front of the incident electromagnetic wave is not too much distorted by atmospheric effects, the phase difference between signals received by different VLBI stations is completely lost. This is because the atmospheric fluctuations at the different antenna sites are uncorrelated, and because the local oscillators in the antennas are not locked by a common phase reference. Fortunately, only phase differences with respect to a reference antenna are important. For a triangle of VLBI antennas, the phase errors due to atmospheric and instrumental fluctuations cancel out in the sum of the phase differences between the antennas of the three baselines involved ("phase closure"). Since the number of baselines scales roughly with the square of the number of antennas, whereas the number of phase errors increases only linearly with it, a considerable part of the phase information can be recovered (e.g., 89 % for the 18 antennas of the EVN). This recovery of phase information can be improved by a "self-calibration" initially assuming a point source as model, calibrating the measured phases under this assumption, and then creating a new source model using an imaging algorithm. In the underlying theory, complex antenna gains are used, and closure relations also exist for their amplitudes.

Such imaging algorithms are needed because the VLBI stations cannot sample the visibility functions on a regular grid of spatial frequencies. Therefore, the brightness distribution resulting from a Fourier transform is convolved with the "synthesized beam," which is the Fourier transform of the sampling of spatial frequencies. Iterative algorithms exist to deconvolve the image such that the result is the brightness distribution as observed with a fictive single dish telescope whose diameter corresponds to the longest available baseline. The CLEAN algorithm (Högbom, 1974) considers the brightness distribution as a collection of spatially unresolved sources. Other deconvolution algorithms have been proposed and applied since then, depending on the nature of the observed brightness distributions. The combination of CLEAN and phase closure is known as hybrid mapping (e.g., Readhead et al., 1980). Global fringe fitting (Schwab and Cotton, 1983) extends the closure relations to time delays and fringe rates and is iteratively used together with a deconvolution algorithm like CLEAN.

For high-precision work (e.g., measurements of the Earth rotation parameters, see below), general relativistic effects need to be considered. As an indication, the gravitational time delay due to the Earth's gravity amounts to up to $\sim$0.02 ns on a 6,000 km long baseline, and the positions of the celestial sources have to be corrected for light bending in the gravitational field of the sun (4 milliarcsecond for an incidence orthogonal to the direction from Earth to Sun, for a summary and further references, see Heinkelmann and Schuh, 2010; Fomalont et al., 2010).

VLBI networks

VLBI networks now extend all over the world. The most sensitive network is the European VLBI Network (EVN), connecting 18 radio telescopes in Europe, Puerto Rico, and South Africa, operating together for more than

3 months per year. The American Very Large Baseline Array (VLBA) works for the whole year. Other national VLBI facilities exist in the UK (the Merlin array), Japan (Japanese VLBI network JVN), and Australia (long baseline array, LBA). Occasionally, some of these networks work together to form global VLBI networks (e.g., the EVN with the VLBA or Merlin, and the Asia-Pacific telescope APT with observatories in Australia, China, New Zealand and Japan). Currently, the best angular resolutions (down to 0.1 milliarcsecond) are achieved with global VLBI at 3 mm wavelength. Future improvements of the spatial resolution scale are to be expected from VLBI below 3 mm wavelength, and from networks including satellite stations (with the Japanese HALCA antenna, in operation from 1997 to 2005, to be replaced by the VSOP 2 mission). These VLBI networks are mainly used for astrophysical research. However, VLBI is also used extensively for geodetic and geophysical applications (see below). Owing to the importance of the VLBI techniques for these disciplines, the International VLBI Service for Geodesy and Astrometry (IVS, Schlüter and Behrend, 2007) coordinates the observations of a dedicated network of VLBI stations on all continents (Figure 2), operated by national research agencies.

Geodetic and geophysical applications

The technique of VLBI is also used for geodetic and geophysical applications. In this context, the positions of compact extragalactic radio sources, like quasars, are considered to be known to sufficient accuracy and the relative telescope coordinates are inferred from time delay observations which reflect the baseline-source geometry. In most cases, networks of six to eight telescopes (Figure 2) are employed in series of weekly sessions organized by the IVS for the determination of Earth orientation parameters (qv *Earth Rotation*) and radio telescope coordinates. Observing between 50 and 60 radio sources in a repeated sequence of scans of 50–100 s duration over a 24-h period provides enough redundancy and geometric stability to determine telescope coordinates and Earth orientation parameters.

Reference systems and tectonics

Geodetic and geophysical applications of VLBI have to do a lot with coordinates of the radio telescopes on Earth and in space. Through sophisticated engineering and constant developments in the theoretical models, the coordinates of radio telescopes around the world can be determined with a relative accuracy of a few millimeters today. These coordinates are always referred to a very specific point of the telescope structure which lies at or close to the intersection of the axes about which the telescope is rotated to aim at the quasars.

The coordinates of geodetically used radio telescopes are determined repeatedly over the years and are fed into the database of the International Earth Rotation and

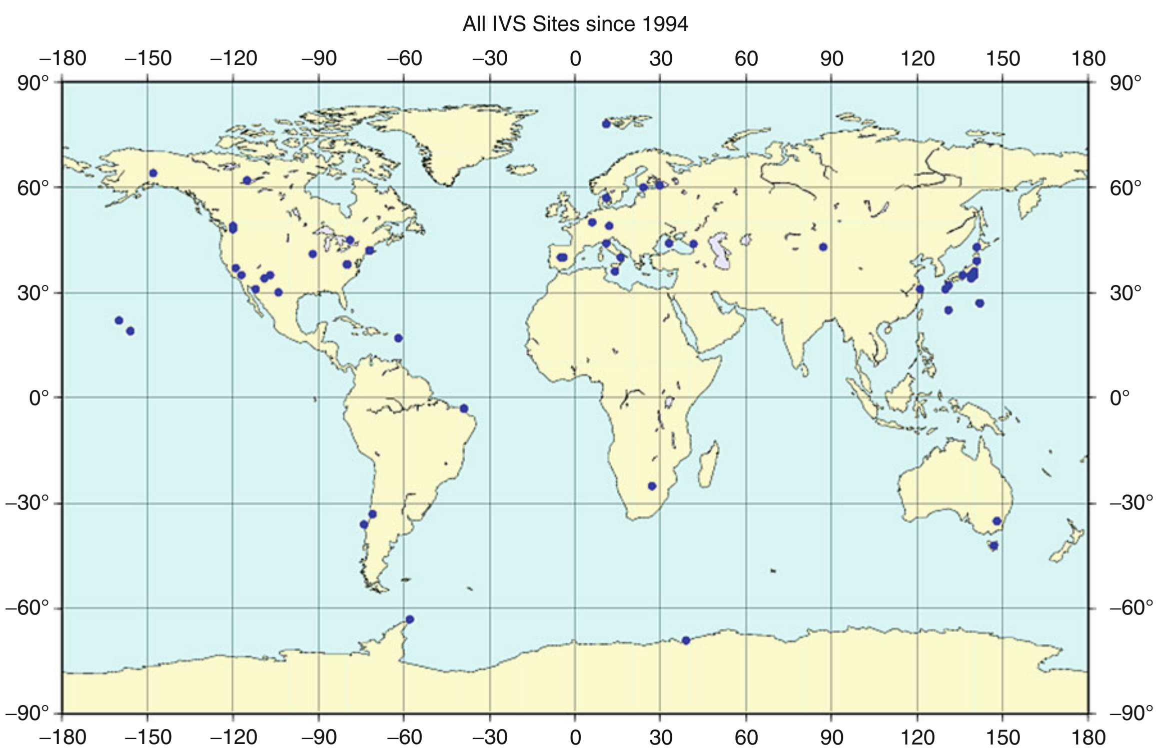

Very Long Baseline Interferometry, Figure 2 Locations of the VLBI antennas of the IVS network participating in the period of 1994 to 2009.

Reference Systems Service (IERS, qv *Earth Rotation*, see also http://www.iers.org). Together with observations of other space-geodetic techniques like the Global Navigation Satellite Systems (GNSS) or Satellite Laser Ranging (SLR, qv *Satellite Laser Ranging*), the VLBI results are merged into the International Terrestrial Reference Frame (ITRF, qv *Geodesy, Networks and Reference Systems*). The last version of the ITRF, ITRF2008, contains about 700 points on Earth which are all accurate to sub-centimeter. The importance of VLBI for this endeavor is that VLBI is the technique which is used to determine the scale of the ITRF. Here, VLBI benefits from the fact that the geodetic VLBI measurements link radio telescopes over intercontinental distances with extreme accuracy. The observations of the other techniques are then used to densify the global reference frame.

Closely linked to the coordinates of the radio telescopes are the changes of the positions which are caused by global tectonics better known as continental drift (qv *Geoid*). Geodetic VLBI was the first technique to verify Alfred Wegener's theory of continental drift through real measurements across the North Atlantic between 1979 and 1984 (Carter et al., 1985; Herring et al., 1986). Today, a full global scenario of several plates and deformation zones exists for which geodetic VLBI has helped to determine the magnitude and direction of the tectonic movements. While the distance between North America and Europe extends by about 20 mm per year, the changes in the Pacific region reach 80 mm per year (Kondo et al., 1987).

Likewise, the positions in space of the Earth and of the quasars observed by VLBI are defined in the International Celestial Reference System (ICRS). The ICRS has been realized through the International Celestial Reference Frame (ICRF, Ma et al., 1998) and its successor, the ICRF2 (Ma et al., 2009), which rely on the VLBI positions of many hundred extragalactic radio sources. Due to the large distances of the latter, the ICRF can be considered as definition of a local inertial system (or quasi-inertial system). The origin of the ICRF is the barycenter of the solar system. Systematic effects and additional random errors of the ICRF2 do not exceed 50–100 microarcseconds (Ma et al., 2009). The accuracy of the ICRF is expected to further improve in the future, thanks to the aforementioned space VLBI (Charlot, 2009).

Earth rotation

Polar motion and irregularities in the Earth's rotation: Geodetic VLBI is one of the few main techniques for the determination and monitoring of the Earth's variable rotation (qv *Earth Rotation*). Through the direct link between the terrestrial and the celestial reference frames, VLBI is the only technique which permits to determine all components of Earth rotation without any input from other techniques. While today polar motion is regularly determined precisely with GPS observations (qv *GPS, Tectonic Geodesy*) on a routine basis, VLBI uniquely contributes the Earth's phase of rotation represented through the time UT1 (Universal Time 1). UT1 is quite variable, due to movements of the atmosphere and of the oceans, and information on UT1 is needed for a number of applications including orbit transformations of Global Navigation Satellite Systems. For this purpose, the International VLBI Service for Geodesy and Astrometry (IVS) runs daily observations providing UT1 with an accuracy of about 5–10 µs.

Precession and Nutation: Looking at the Earth's axis of rotation in space, one can see that it describes a cone with an opening angle of 23.45°, which needs about 25,700 years to complete. This phenomenon is called precession. Superimposed on the precession cone are periodic movements of the Earth's axis of rotation which have a magnitude of a few arcseconds and are called nutation. For historical reasons, precession and nutation are handled independently although they are caused by the same phenomenon: The astronomical bodies of Sun, Moon, and planets exert a torque on the equatorial bulge of the Earth trying to pull it toward the ecliptic. Through its desire to conserve angular momentum, the Earth reacts with a precession effect. Through the periodic rotations of the attracting bodies, superimposed periodicities result and more than a 1,000 nutation periods can be identified covering a spectrum from 13.6 years down to a few days.

General relativistic effects in Earth Rotation: Owing to the orbital motion of the Earth, spin-orbit coupling leads to a "geodetic precession" of about 2 arcseconds per century (qv *Earth Rotation*, Klioner et al., 2010) that are measured by VLBI, which lends itself also to other tests of general relativity (Fomalont et al., 2010).

Today, geodetic VLBI is the only technique that is used to determine precession and nutation. The accuracy of the nutation offsets determined from 24 h of VLBI observations is on the order of 80–100 microarcseconds which correspond to about 3 mm when transformed to a metric displacement at the Earth's surface. The agreement between these observations and a model which is derived geophysically using an elastic Earth model is on the order of 1 milliarcsecond. The main cause of the deviations is the effect of the so-called free core nutation (FCN). This phenomenon results from the fact that the Earth's core has a slightly different ellipticity than the rest of the body resulting in different torques.

Bibliography

Bare, C., Clark, B. G., Kellermann, K. I., Cohen, M. H., and Jauncey, D. L., 1967. Interferometer Experiment with Independent Local Oscillators. *Science*, **157**, 189–191.

Carter, W. E., Robertson, D. S., and Mackay, J. R., 1985. Geodetic radio interferometric surveying: Applications and results. *Journal of Geophysical Research*, **90**, 4577–4587.

Charlot, P., 2009. Space VLBI and the radio reference frame. In Hagiwara, Y., et al. (eds.), *Approaching micro-arcsecond resolution with VSOP-2: Astrophysics and technologies*. ASP Conference Series, Vol. 402, pp. 480–485.

Fomalont, E., Kopeikin, S., Jones, D., Honma, M., and Titov, O., 2010. Recent VLBA/VERA/IVS tests of general relativity. In

Klioner, S. A., Seidelmann, P. K., and Soffel, M. H. (eds.), *Relativity in Fundamental Astronomy*. Cambridge: Cambridge University Press, pp. 291–295.
Garrett, M. A., Porcas, R. W., Pedlar, A., Muxlow, T. W. B., and Garrington, S. T., 1999. Wide-field VLBI imaging. *New Astronomy Reviews*, **43**, 519–522.
Heinkelmann, R., and Schuh, H., 2010. Very long baseline interferometry: accuracy and relativistic tests. In Klioner, S. A., Seidelmann, P. K., and Soffel, M. H. (eds.), *Relativity in Fundamental Astronomy*. Cambridge: Cambridge University Press, pp. 286–290.
Herring, T. A., Shapiro, I. I., Clark, T. A., Ma, C., and Ryan, C., 1986. Geodesy by radio interferometry: Evidence for contemporary plate motion. *Journal of Geophysical Research*, **91**, 8341–8347.
Högbom, J. A., 1974. Aperture synthesis with a non-regular distribution of interferometer baselines. *Astronomy & Astrophysics Supplement*, **15**, 417–426.
Klioner, S. A., Gerlach, E., and Soffel, M. H., 2010. Relativistic aspects of rotational motion of celestial bodies. In Klioner, S. A., Seidelmann, P. K., and Soffel, M. H. (eds.), *Relativity in Fundamental Astronomy*. Cambridge: Cambridge University Press, pp. 112–123.
Kondo, T., Heki, K., and Takahashi, Y., 1987. Pacific plate motion detected by the VLBI experiments conducted in 1984-1985. *Radio Research Laboratories Journal*, **34**, 1–14.
Ma, C., Arias, F., Bianco, G., Boboltz, D., Bolotin, S., Charlot, P., Engelhardt, G., Fey, A., Gaume, R., Gontier, A.-M., Heinkelmann, R., Jacobs, C., Kurdubov, S., Lambert, S., Malkin, Z., Nothnagel, A., Petrov, L., Skurikhina, E., Sokolova, J., Souchay, J., Sovers, O., Tesmer, V., Titov, O., Wang, G., Zharov, V., Böckmann, S., Collioud, A., Gipson, J., Gordon, D., Lytvyn, S., MacMillan, D., and Ojha, R., 2009. *The Second Realization of the International Celestial Reference Frame by Very Long Baseline Interferometry (IERS Technical Note 35)*. Frankfurt am Main, Germany: Verlag des Bundesamtes für Kartographie und Geodäsie.
Ma, C., et al., 1998. The International Celestial Reference Frame as realized by very long baseline interferometry. *Astronomical Journal*, **116**, 516–546.
Readhead, A. C. S., Walker, R. C., Pearson, T. J., and Cohen, M. H., 1980. Mapping radio sources with uncalibrated visibility data. *Nature*, **295**, 137–140.
Ryle, M., and Vonberg, D. D., 1946. Solar radiation at 175 Mc/s. *Nature*, **158**, 339–340.
Schlüter, W., and Behrend, B., 2007. The International VLBI Service for Geodesy and Astrometry (IVS): current capabilities and future prospects. *Journal of Geodesy*, **81**, 397–387.
Schwab, F. R., and Cotton, W. D., 1983. Global fringe search techniques for VLBI. *Astronomical Journal*, **88**, 688–694.
Sudarshan, E. C. G., 1963. Equivalence of semiclassical and quantum mechanical descriptions of statistical light beams. *Physical Review Letters*, **10**, 277–279.
Tornatore, V., and Charlot, P., 2007. The impact of radio source structure on European geodetic VLBI measurements. *Journal of Geodesy*, **81**, 469–478.
van Cittert, P. H., 1934. Die wahrscheinliche Schwingungsverteilung in einer von einer Lichtquelle direkt oder mittels einer Linse beleuchteten Ebene. *Physica*, **1**, 201–210.
Zernike, F., 1938. The concept of degree of coherence and its application to optical problems. *Physica*, **5**, 785–795.

Cross-references

Earth Rotation
Geodesy, Networks and Reference Systems
Geoid
GPS, Data Acquisition and Analysis
GPS, Tectonic Geodesy
SAR Interferometry
Satellite Laser Ranging

Springer

http://www.springer.com/978-90-481-8701-0

Encyclopedia of Solid Earth Geophysics
NGRI, D. (Ed.)
2011, LXXIV, 1539 p. In 2 volumes, not available
separately., Hardcover
ISBN: 978-90-481-8701-0